Magic Angle Spinning Dynamic Nuclear Polarization Solid-State NMR Spectroscopy of γ-Irradiated Molecular Organic Solids

*Scott L. Carnahan[1,2], Yunhua Chen[1,2], James F. Wishart[3], Joseph W. Lubach[4], and Aaron J. Rossini[1,2]**

[1] US DOE Ames Laboratory, Ames, Iowa, USA, 50011

[2] Iowa State University, Department of Chemistry, Ames, IA, USA 50011

[3] Brookhaven National Laboratory, Chemistry Division, Upton, New York 11973, United States

[4] Genentech Inc., South San Francisco, California 94080, United States

AUTHOR INFORMATION

Corresponding Author

*e-mail: arossini@iastate.edu, phone: 515-294-8952.

ABSTRACT

In the past 15 years, magic angle spinning (MAS) dynamic nuclear polarization (DNP) solid-state has emerged as a method to increase the sensitivity of high-resolution solid-state NMR spectroscopy experiments. Recently, γ-irradiation was used to generate significant concentrations of homogeneously distributed free radicals in a variety of solids. Both γ-irradiated quartz and glucose showed significant MAS DNP enhancements. Here, γ-irradiation is applied to twelve small organic molecules to test the applicability of γ-irradiation as a general method of creating stable free radicals for MAS DNP experiments on organic solids and pharmaceuticals. Concentrations of radicals in the range of 0.25 mM to 10 mM were observed in irradiated glucose, histidine, malic acid, and malonic acid, and significant ^{1}H DNP enhancements of 32, 130, 19, and 11 were obtained, respectively, as measured by ^{1}H→^{13}C CPMAS experiments. However, concentrations of free radicals below 0.05 mM were generally observed in organic molecules containing aromatic rings, preventing sizeable DNP enhancements in those molecules. DNP sensitivity gains for several of the irradiated compounds exceed that which can be obtained with the relayed DNP approach that uses exogeneous polarizing agent solutions and impregnation procedures. In several cases, significant ^{1}H DNP enhancements were realized at room temperature. This study demonstrates that in many cases γ-irradiation is a viable alternative to addition of stable radicals for DNP experiments on organic solids.

Graphical Abstract

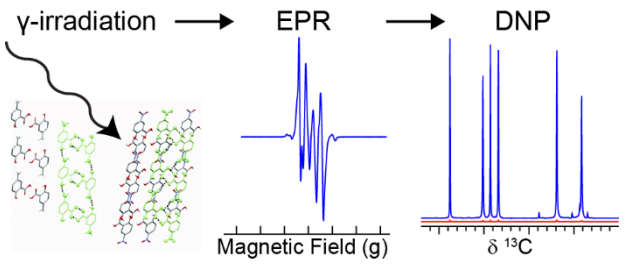

Introduction

Solid-state nuclear magnetic resonance (SSNMR) spectroscopy is a powerful technique for probing the structure and dynamics of both amorphous and crystalline solids. However, NMR is an intrinsically insensitive technique, primarily due to the minute differences in the Boltzmann population of the nuclear spin states. The sensitivity of SSNMR spectroscopy is further reduced because many NMR-active nuclei of interest have low natural isotopic abundance (*e.g.*, ^{13}C, ^{15}N, ^{17}O, *etc.*), longitudinal relaxation time constants (T_1) are often on the order of minutes or hours in the solid-state, and a variety of mechanisms lead to broadening of solid-state NMR signals.

Due to the efforts of Griffin and co-workers, magic angle spinning (MAS) dynamic nuclear polarization (DNP) has emerged as a technique that can routinely increase the sensitivity of SSNMR experiments by one to two orders of magnitude.[1-5] MAS DNP has been used to enhance sensitivity and enable multi-dimensional solid-state NMR experiments on samples such as nanomaterials,[6-8] biosolids,[9-14] pharmaceuticals,[15-18] and inorganic solids.[19-24] MAS DNP experiments require the presence of unpaired electron spins that can serve as the source of enhanced nuclear spin polarization. The most common technique for introducing the necessary unpaired electrons into the sample is to impregnate the sample with or dissolve it in a suitable solution (*e.g.* glycerol/water, tetrachloroethane, etc.) containing exogeneous polarizing agents that

usually contain nitroxide groups (*e.g.* TOTAPOL, TEKPOL, AMUPol, *etc.*),[6] although, other types of radicals are also known.[6, 25-27] Unfortunately, some materials are sensitive towards the solvents and/or polarizing agents. For example, impregnation of theophylline and other pharmaceuticals with solvents used for DNP experiments was observed to cause polymorphic phase transformations.[15, 18] Reactions between free radicals and various samples have also been observed.[28-35] Another potential problem arises when the analyte is insoluble in the radical solution. In such cases, the radicals will be restricted to the surface of the material, resulting in preferential enhancement of surface NMR signals, which is often a desirable feature of MAS DNP experiments.[4, 30, 36-37] In favorable cases, nuclear spin diffusion may relay polarization from the surface to sub-surface or bulk spins;[21, 24, 38-39] however, hyperpolarization of nuclear spins in the bulk is limited by the spin diffusion rate and longitudinal nuclear spin relaxation, both of which are intrinsic properties of the material under study. For all of these reasons, there is a need for alternative approaches to prepare materials for DNP experiments that can eliminate the need for solvents and exogeneous polarizing agents and more efficiently polarize the bulk region of materials.

An alternative to the addition of an exogenous polarizing agents is to use endogenous free radicals or to directly introduce a radical source within the bulk of the sample. Previously, DNP has been performed on materials that contain intrinsic radical centers such as silicon,[34, 40-44] coal,[45-46] diamond,[47-48] and various metals/conductors.[49-50] Another technique is to synthetically dope the samples with a radical, either with an EPR-active metal ion (*e.g.*, Mn^{2+}, Gd^{3+}, Cr^{3+}, *etc.*)[22, 51-59] or by tethering a nitroxide radical to the analyte.[30, 32, 60-64] However, these approaches often require synthetic modification of each sample on a case by case basis. Significant concentrations of free radicals have previously been introduced into organic solids by using electrical discharge[65-66] or

ionizing radiation,[67-73] with several of these studies also describing DNP experiments on the irradiated materials. In fact, there is a long history of small organic molecules such as alanine and sucrose being used as EPR-based radiation dosimeters.[70, 74-79] Neutron-, electron beam-, or γ-irradiated organic solids were utilized for some of the earliest DNP NMR experiments at low fields, ultra-low temperatures, and without sample rotation.[80-84] Recently, we showed that high-field MAS DNP could be performed on γ-irradiated glucose and quartz.[85] MAS DNP enhancements of 400 and 36 were realized for direct excitation ^{29}Si NMR of quartz and ^{1}H→^{13}C cross polarization (CP) NMR of glucose, respectively. The large enhancements in quartz allowed a natural abundance ^{29}Si-^{29}Si refocused INADEQUATE experiment. DNP enhancements of *ca.* 120 were even seen at room temperature for γ-irradiated quartz. Perras *et al*. were able to accurately calculate the ^{29}Si DNP enhancement of γ-irradiated quartz using an *ab initio* computational framework that takes into account spin diffusion between thousands of ^{29}Si atoms.[86]

Here, we investigate the generality of γ-irradiation to create stable radicals in organic samples of relevance to pharmaceutical science. A variety of γ-irradiated organic solids were found to possess mM concentrations of free radicals and exhibited sizable ^{1}H MAS DNP signal enhancements. We discuss limitations and benefits intrinsic to this method and compare the sensitivity of DNP-enhanced solid-state NMR experiments on irradiated materials and traditional impregnated samples. In several cases DNP sensitivity gains for the irradiated compounds exceed that which can be obtained with exogeneous polarizing agents and impregnation procedures. Importantly, for several γ-irradiated organic solids significant DNP enhancements were obtained at room temperature.

Results and Discussion:

Samples. The small organic molecules chosen for this study can be fit into two categories: samples without and with aromatic rings (Figure 1). These materials have an array of uses, such as food additives, pharmaceutical excipients, and drugs. The two cocrystals of the pharmaceutical denoted GDC-022 (fumaric acid and phosphoric acid) were designed for treatment of autoimmune diseases.[18] Samples were chosen such that they covered a diverse set of chemical structures to investigate the generality of γ-irradiation to create stable free radicals for MAS DNP.

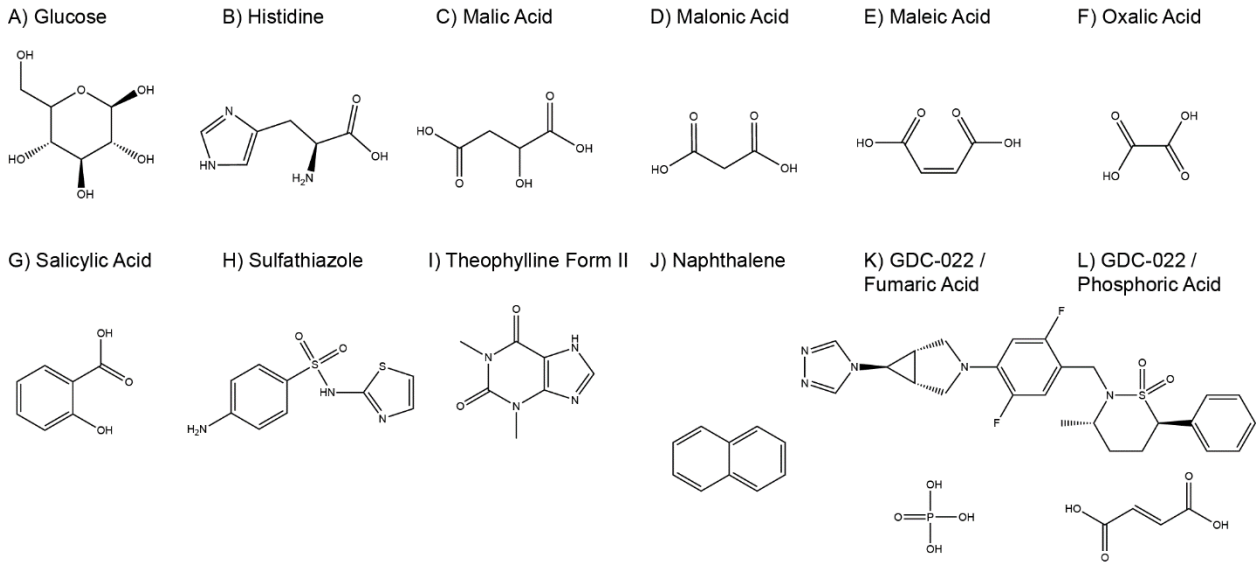

Figure 1. Chemical structures of organic compounds in this study.

γ-Irradiation. Each of the molecules in Figure 1 was subjected to the same standard procedure: 1) the powdered solids were γ-irradiated at Brookhaven National Laboratory to generate free radicals, 2) X-band electron paramagnetic resonance (EPR) was used to determine the concentration of radicals and provide insight into their identity and 3) for samples showing significant amounts of free radicals MAS DNP NMR experiments were performed. Throughout the entire process the samples were handled in air. The compounds were γ-irradiated using a Co-60 source which can accommodate up to 4 samples at a time. The dose rate of γ-irradiation was

ca. 6.1 kGy/hr on this system and the samples are typically irradiated for 4 hours. The exception is histidine hydrochloride monohydrate, which was γ-irradiated at *ca.* 8 kGy/hr for 4 hours. Recently, we have shown that γ-irradiated quartz and glucose are amenable to the creation of stable radicals suitable for MAS DNP.[85] Quartz and glucose required different amounts of irradiation necessary to create the optimal DNP conditions. After a *ca.* 32 kGy dose of γ-irradiation, glucose had the highest radical concentration without sacrificing any NMR linewidth.[85] Consequently, a 24 kGy dose of γ-irradiation was chosen as the standard amount of radiation for the series of organic solids tested here. The only exception is that the glucose used for the room-temperature DNP experiment was γ-irradiated with a *ca*. 17.5 kGy dose.

Electron Paramagnetic Resonance Spectroscopy. After γ-irradiation, the samples were shipped back to Iowa State University and analyzed using continuous-wave (CW) EPR to determine radical concentration (Figure 2). Radical concentrations and the field setting were calibrated using a standard sample of γ-irradiated quartz.[85, 87-88] Previously, γ-irradiated glucose was determined to possess a 1-4 mM concentration radicals, depending on the dose of radiation.[85] Of the 11 γ-irradiated samples tested here, malic acid and malonic acid had comparable or higher radical concentrations as compared to glucose, while the rest had sub-mM radical concentrations (Figure 2, Table 1). In addition, malic and malonic acids had higher radical concentrations as compared to the related maleic and oxalic acids, which both have only unsaturated carbon atoms. All of the dicarboxylic acids showed complex EPR spectra with hyperfine couplings from proton spins dominating the spectrum. For the samples containing phenyl groups or aromatic rings, they all had fairly low radical concentrations and typically had a broad featureless peak in the EPR spectrum. Salicylic acid is one notable exception of an aromatic compound that shows some larger hyperfine couplings. Many of the γ-irradiated samples tested here have been previously studied by

EPR spectroscopy, with a summary of the previously proposed radical species summarized in the Supplemental Information (Figure S1) and further discussed below.[89-101]

Generally speaking, transfer of energy from the incident ionizing (gamma) radiation causes an electron to be ejected from a molecule in the sample, leaving behind a molecular cation radical bearing a "hole", or electron vacancy. Within a few picoseconds or less, the molecular cation radical transfers a proton to a neighboring molecule to become a neutral molecular radical that is subsequently detected in our experiments. The other product is a closed-shell protonated molecular cation that is not detectable in this experiment. The ejected electron typically has 10-100 eV of excess kinetic energy, so it comes to rest some distance away from the hole. Although the kinetics are slow in the solid phase, a large fraction of the initially-formed electrons and holes are subsequently annihilated via recombination, but generally speaking there is no path that leads to biradicals. Therefore, there is no reason to believe that γ-irradiation creates radical pairs or clusters of free radicals in most cases. However, oxalic acid dihydrate is hypothesized to form a biradical upon irradiation (see below).

γ-irradiated glucose is proposed to have two stable carbon-centered radicals, denoted RI-A and RII-C.[89-101] γ- and X-ray irradiation of histidine hydrochloride monohydrate was proposed to lead to formation of a carbon-centered radical via deamination.[92] Malic acid is known to lose a hydroxide during γ-irradiation.[97] The CH_2 group of malonic acid loses a hydrogen atom during γ-irradiation,[96] although other radicals are seen at low temperature.[94] Maleic acid is proposed to form a radical of the form HOOC-H2C-•CH-COOH during irradiation at room temperature,[90] although carboxyl and vinyl radicals are seen to form when irradiated by either γ- or X-rays at 77 K.[91] γ-irradiated oxalic acid dihydrate forms the oxalate biradical, and the hyperfine splittings come from the waters of hydration.[93, 101] While no report was found for studying the impact of γ-, electron

beam, or X-ray irradiation on salicylic acid, it is known to produce small amounts of radicals when exposed to either heat[100] or UV light.[99] Four different radicals were proposed for formation under γ-irradiation for sulfathiazole, although there is no strong evidence for any of them.[95] Theophylline was shown to be stable against radical formation upon electron beam irradiation.[98] Naphthalene, as well as many other aromatic compounds, is fairly unresponsive to γ-irradiation.[89] It is well known that aromatic rings can absorb the radiolytic energy from γ-irradiation, resulting in excitation instead of ionization, explaining why only low radical concentration were observed in these materials.[89, 102-104] Ionizing radiation with a higher linear energy transfer (LET) such as ^{1}H, ^{4}He, or ^{12}C heavy ion irradiation are known to produce higher yields of H_2 in aromatic samples,[104] suggesting a possible path forward to introducing higher concentrations of radicals for DNP in aromatic molecular solids.

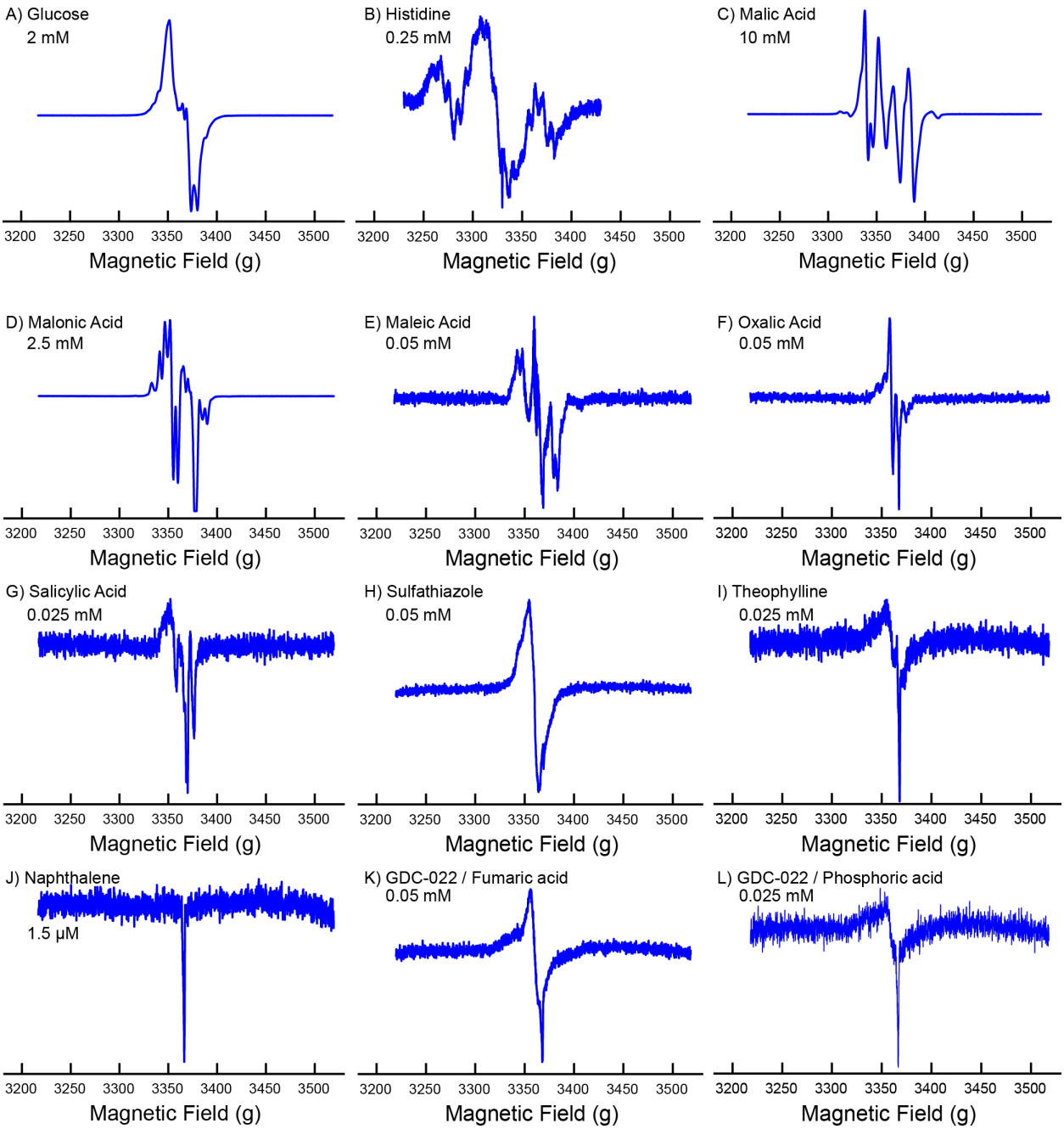

Figure 2. Room temperature continuous-wave X-band EPR spectra of γ-irradiated organic molecules. The concentration of free radicals is indicated next to each spectrum.

Dynamic Nuclear Polarization NMR. In order to perform DNP with a fixed frequency gyrotron the field of the NMR magnet must be adjusted to enable microwave irradiation to occur at the correct part of the EPR spectrum. Typically, the magnetic field is set to obtain positive maximum ^{1}H DNP enhancements with nitroxide biradicals (set as 0 ppm in Figure 3, which

approximately corresponds to $g = 2.004$).[105] Carbon-centered radicals typically have an isotropic g-value of *ca*. 2.002, therefore if the cross-effect (CE) is the dominant DNP mechanism, we anticipate that the optimal magnetic field value for DNP must be increased as compared to the optimal field value for nitroxide radicals. Indeed, the DNP field sweep profiles of all γ-irradiated samples studied showed broad matching conditions, with maxima in the DNP enhancements obtained at a higher magnetic field than is used for nitroxide radicals (Figure 3). Interestingly, all of the samples for which a field sweep was performed had a maximum near +1600 ppm (9.418 T), which approximately corresponds to microwave saturation at $g \sim 2.001$-2.000, *i.e.*, on resonance saturation of carbon centered radicals. This is promising in that a field sweep may not be necessary for all samples, which drastically improves the throughput of the experiments since field sweep DNP experiments are generally very time consuming. For several samples (maleic acid, oxalic acid, sulfathiazole, salicylic acid, and the GCD-022 cocrystals), no field sweep was performed and the samples were tested with the magnetic field offset of *ca*. +1600 ppm. Despite the lack of a full field sweep profile, maleic acid and oxalic acid each had large DNP enhancements (Figure 4 and Table 1).

Considering the breadth of the DNP field sweep profiles, the observation of negative DNP enhancements that are similar in magnitude to positive DNP enhancements (Figure 2 and Figure S2), and the fact that DNP enhancements are maximized when microwave saturation occurs on resonance with the electron spins, we conclude that the cross effect (CE) must be the primary DNP mechanism active in these samples.[1] The CE requires dipole-coupled electron spins. For example, the CE is optimized for nitroxide monoradicals dissolved in frozen solution when the radical concentration is around 40 mM. Therefore, it is somewhat surprising to see significant DNP enhancements in many irradiated solids considering that γ-irradiation is primarily hypothesized to

yield monoradicals (see Figure S1 and discussion above) and the radical concentrations are less than 4 mM in all samples. Therefore, DNP is likely driven in the irradiated solids by a small fraction of radical centers that happen to be proximate to another radical center to enable the CE. This hypothesis could explain why only solids with long ^{1}H T_1 show sizeable DNP enhancements; in solids with shorter ^{1}H T_1, the time for ^{1}H spin diffusion of hyperpolarization from CE active radical pairs and for accumulation of hyperpolarization will be limited.[17, 21, 38, 39, 55, 57]

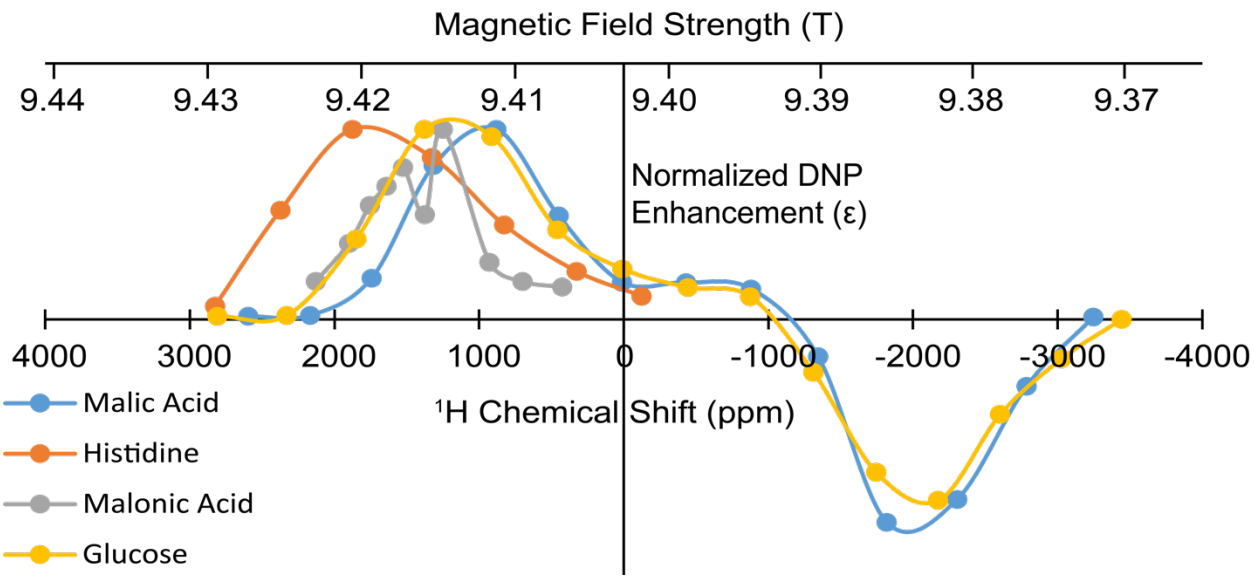

Figure 3. DNP field sweep profiles for malic acid (blue), glucose (yellow), histidine (orange), and malonic acid (gray). DNP enhancements were normalized to fit on the same scale. The magnetic field offset of 0 ppm corresponds to the field setting that gives a positive maximum DNP enhancement with nitroxide biradicals.

Large ^{1}H→^{13}C CP DNP enhancements were obtained for a number of γ-irradiated organic samples (Figure 4, Table 1). Enhancements from malic acid (ε = 19), malonic acid (ε = 11), and oxalic acid (ε = 67) were comparable to the enhancements for γ-irradiated glucose (ε = 32). A DNP enhancement of at least 144 was realized for γ-irradiated maleic acid and 130 for γ-irradiated histidine. However, several of the samples exhibited low or no DNP enhancements (sulfathiazole, salicylic acid, GDC-022 fumaric acid cocrystal, and GDC-022 phosphoric acid cocrystal). These

samples are ones that had low radical concentrations and no detailed DNP field sweep was performed. Some also had relatively short ^{1}H T_1, on the order of tens of seconds. The lack of DNP enhancements in these samples is not surprising as there is a minimum number of radicals necessary for DNP to be effective, as discussed above. One point of note is that the ^{1}H DNP build-up time (T_{DNP}) or ^{1}H T_1 (measured without microwave irradiation) is clearly an important factor in the magnitude of the DNP enhancement. Samples with longer T_1/T_{DNP} had the largest enhancements (histidine, oxalic acid, and maleic). Even sulfathiazole and salicylic acid, which had low radical concentrations, exhibited minor DNP enhancements due to their long T_1. Impregnation and relayed DNP is likely the superior method for those samples.[38, 106]

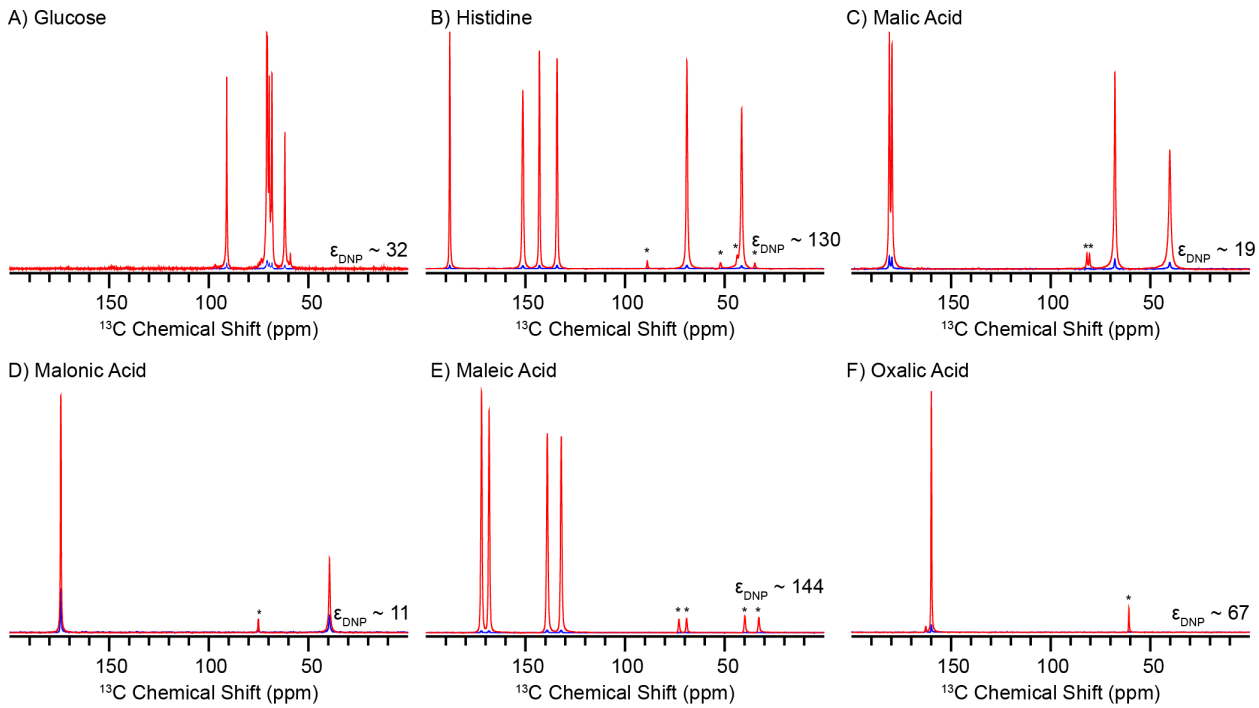

Figure 4. ^{1}H→^{13}C CPMAS solid-state NMR spectra of several γ-irradiated organic compounds. Spectra were obtained with microwaves to drive DNP (red) or without DNP (blue). DNP enhancements are indicated. Spinning sidebands are denoted asterisks.

Table 1: Radical concentrations, Relaxation Time Constants, $^{1}H \rightarrow ^{13}C$ CPMAS DNP Enhancements and ^{13}C NMR Sensitivity for Experiments Performed at 100 K.

Sample	Radical Concentration (mM)	T_{DNP} (s)[a]	T_1 (s)[a]	ε_{DNP}[b]	S_{13C} ($min^{-1/2}$)
Glucose -γ-irrad	2	130	-	32	155
Glucose -TEKPOL/TCE	32	350	-	30	48
Malic Acid -γ-irrad	10	50	70-120	19	446
Malic Acid -TEKPOL/TCE	32	500	2,800	26	95
Malic Acid -No radicals	0	-	2,000	-	5
Histidine HCl H_2O -γ-irrad	0.25	900	-	130	539
Histidine HCl H_2O -TEKPOL/TCE	32	350	1,400	18	75
Malonic Acid -γ-irrad	2.5	40	46	11	741
Malonic Acid -No radicals	0	-	200	-	30
Oxalic Acid -γ-irrad	0.05	>9,000	-	67	184
Maleic Acid -γ-irrad	0.05	>5,000	-	144-240	414
Sulfathiazole -γ-irrad	0.05	>1,400	>1,000	2.4	4
Salicylic Acid -γ-irrad	0.025	>20,000	-	6	10
GDC-022 Fumaric Acid cocrystal -γ-irrad	0.05	20	30-50	1	5
GDC-022 Phosphoric Acid cocrystal -γ-irrad	0.025	15	170	2	6
Theophylline Form II	0.025				
Naphthalene	0.00015				

[a] T_{DNP} was measured with DNP-enhanced saturation recovery experiments. T_1 was measured with saturation recovery experiments without DNP and, where indicated, on samples which did not contain any radicals. All saturation recovery curves were adequately fit with mono-exponential functions, despite the fact that signal build-up is likely multi-exponential. However, for samples with T_{DNP}/T_1 values on the order of thousands of seconds it is challenging to measure spectra with delays of 3-5 $\times T_1$. Therefore, there is likely a significant uncertainty in the larger T_1/T_{DNP} values.
[b] ^{13}C CPMAS spectra obtained with and without microwave irradiation are shown in Figures S8-S11 for sulfathiazole, salicylic acid, GDC-022 / fumaric acid cocrystal and GDC-022 / phosphoric acid cocrystal.

We evaluated the effectiveness of radicals created by γ-irradiation for DNP with the following two criteria: 1) the radicals created by γ-irradiation must be stable over the long term (weeks or months) and 2) the sensitivity and resolution of the DNP-enhanced ^{13}C CPMAS SSNMR spectra obtained from irradiated materials should be comparable to the spectra obtained from the same material prepared by incipient wetness impregnation (IWI)[37-38] technique.

To the first point, EPR spectroscopy indicates that a sample of γ-irradiated histidine had no reduction in radical concentration over the course of storage for two years at room temperature in air (Figure S3). Likewise, we previously observed that the free radicals of γ-irradiated glucose were similarly long-lived.[85] Although we have not investigated all materials in detail, we have the sense that the free radicals in nearly all γ-irradiated solids are stable for months if not years. For example, the samples of γ-irradiated glucose we used for experiments here was originally γ-irradiated in 2017 and was stored in a refrigerator when not in use.

There is a factor of 3-6 overall gain in NMR sensitivity (S = signal-to-noise ratio × (experiment time)$^{-1/2}$) for three of the γ-irradiated samples tested (glucose, histidine, and malic acid, Table 1, Figure S4-S7) as compared to spectra obtained from samples prepared by the standard IWI method. Impregnated histidine is frequently used as a setup sample for DNP experiments in our laboratory. A detailed discussion on the reproducibility of the sensitivity in a sample of IWI histidine over the course of more than 20 sample formulations can be found in Figure S12. As compared to the IWI method, there is a minor broadening in the baseline of a couple of samples, mainly noticeable in γ-irradiated samples with higher radical concentration, such as malic acid (Figure 5C) and glucose γ-irradiated with a 81 kGy dose.[85] Malonic acid also showed broadening in the baseline of peaks as compared to a sample without the addition of radicals (Figure S6). The broadening is most likely from ^{13}C in the vicinity of the radical defects.

Comparing malic acid and malonic acid before and after γ-irradiation shows that DNP on the irradiated materials provides 90-200 times improved sensitivity, showing the utility of DNP (Figures S5 and S6). The introduction of radicals, both from γ-irradiation and IWI, also reduces the T_1 of the sample. For example, in malic and malonic acid the T_1 (measured without DNP) decreases by approximately 5-10 times due to γ-irradiation. T_{DNP} is shorter than the T_1 due to ^{1}H homonuclear spin diffusion and sample heating during the application of the microwaves,[38, 107] which may account for the slight perceived enhancement in sulfathiazole, salicylic acid, or the GCD-022 / phosphoric acid cocrystal. Reducing the T_1 or T_{DNP} allows scans to be performed more rapidly, which naturally increases the sensitivity.

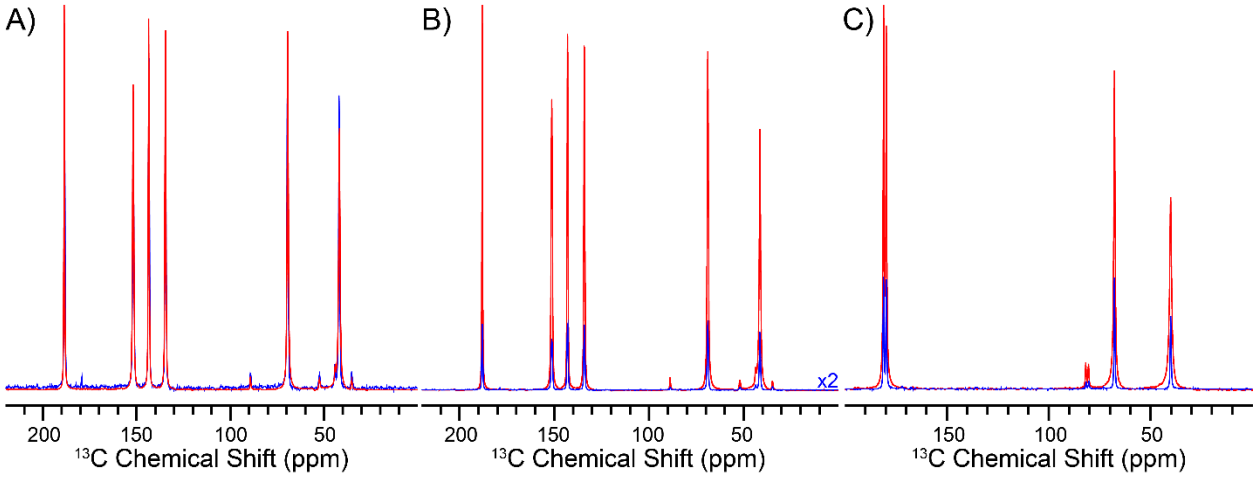

Figure 5. A) Comparison of linewidths for γ-irradiated histidine (red) with IWI DNP histidine (blue) impregnated with 16 mM TEKPOL in TCE. Spectra are scaled to the same intensity to illustrate the similarity of the linewidths. B) Comparison of intensity for γ-irradiated histidine (red) and histidine impregnated with 16 mM TEKPOL in TCE (blue). The spectra of the γ-irradiated and IWI sample were obtained with 1 scan and recycle delays of 1000 s and 500 s. The intensity for the IWI sample is scaled by 2 to account for the difference in recycle delays. C) Comparison of intensity for γ-irradiated malic acid (red) with IWI DNP malic acid (blue) impregnated with 16 mM TEKPOL in TCE.

Room-temperature DNP. To date there have only been a few instances of room-temperature MAS DNP.[45, 49, 108] In general, for MAS DNP to succeed, the electron and nuclear spins need to be hosted in a rigid lattice that affords long nuclear and electron relaxation time

constants; at room temperature, many solids exhibit rotational or translational motions that result in reduced nuclear and electron relaxation times. We showed that γ-irradiated quartz had room-temperature ^{29}Si DNP enhancements of approximately 120,[85] likely because quartz is a rigid solid at room temperature, which results in long electron and nuclear T_1. Likewise, Hope, Emsley, Grey and co-workers observed ^{17}O DNP enhancements of 320 at room temperature for Gd-doped ceria.[109]

Here, we tested room-temperature MAS DNP on four of the γ-irradiated samples that showed the highest DNP enhancements at 100 K: maleic acid, malic acid, glucose, and oxalic acid. Of them, three showed significant room-temperature DNP enhancements (Table S1) with the best enhancement of 8 obtained with maleic acid, while enhancements of 4 and 1.6 were measured for malic acid and glucose, respectively. Of the three, maleic acid had the longest ^{1}H T_1 at room temperature (Table S1), likely explaining why it provided the largest DNP enhancements.

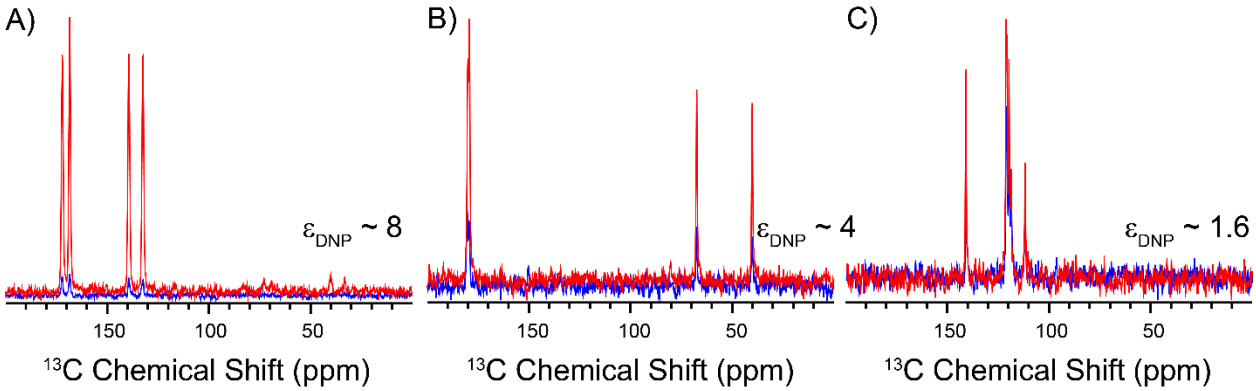

Figure 6. Room-temperature MAS DNP of γ-irradiated (A) maleic acid, (B) malic acid, (C) and glucose.

Conclusions

In conclusion, we have shown that γ-irradiation can create μM to mM concentrations of stable free radicals in a variety of organic solids, consistent with the observations of prior studies.[67-73] In many of the γ-irradiated organic solids the radicals can be used for indirect DNP $^{1}H \rightarrow ^{13}C$ CPMAS experiments. Despite the relatively low radical concentrations, significant ^{1}H DNP enhancements were realized in histidine, salicylic acid, and sulfathiazole. Higher absolute NMR sensitivities were observed for several of the irradiated solids as compared to relayed DNP experiments on samples prepared with IWI of nitroxide biradical solutions. Therefore, γ-irradiation can potentially provide significant DNP enhancements and NMR sensitivity gains in organic molecules without the need for sample grinding to reduce particle sizes or the introduction of exogenous solvents or radicals to the sample, steps which can cause unwanted phase transformations in some instances.[15,18] Importantly, significant room-temperature ^{1}H DNP enhancements were realized for γ-irradiated maleic acid, malic acid and glucose.

The most significant weakness of using γ-irradiation for creating radicals is that it does not consistently create a high concentration of radicals in all compounds tested. Furthermore, limited access to γ-irradiation sources is also a hindrance. However, stable free radicals in organic solids could also possibly be obtained with X-ray irradiators or medium-energy (1-10 MeV) electron accelerators. While high energy radiation sources are not standard laboratory equipment, they can often be found in university science departments or medical centers, and are in industrial use for sterilization and polymer curing or modification systems. Future studies should investigate the use of other high energy photon/particle sources to create stable free radicals for DNP.

Samples with aromatic rings proved more resistant to forming stable radicals, most likely due to the radiolytic energy being mostly funneled into excited states of the aromatic ring or

through electron-hole recombination. In a few of the samples no DNP enhancement was observed, likely due to the combination of radical concentrations below 0.05 mM and/or T_{DNP}/T_1 shorter than 60 s. Further study is needed to determine if different types of ionizing radiation, such as heavy ion irradiation, could be used to increase radical concentrations in aromatic compounds.[104] For samples with low radical concentrations and/or intrinsic T_1 values below 100 s, MAS DNP at temperatures below 70 K using helium for sample cooling could provide a way to increase the increase DNP enhancements by prolonging ^{1}H T_1.[110-114]

Experimental

Materials. Glucose, malonic acid, maleic acid, malic acid, salicylic acid, oxalic acid, and sulfathiazole were purchased from Sigma-Aldrich Inc. and used without further purification. Histidine hydrochloride monohydrate (histidine) was purchased from Chem-Impex International Inc. The GDC-022 API cocrystal formulations were provided by Genentech Inc.[18] Irradiated organic solids were kept in the refrigerator, except for histidine, which was kept in a drawer at room temperature. Even at room temperature, there was no sign of a loss of radicals even over the course of 1.5 years for irradiated histidine (Figure S2).

γ-Irradiation of Materials. All samples were gamma-irradiated using the Co-60 source of the Accelerator Center for Energy Research (ACER) at Brookhaven National Laboratory, as described in reference 85. The dose rate was approximately 6.1 kGy/hr.

EPR Spectroscopy. Room temperature X-band CW EPR was performed on an ELEXSYS E580 EPR system. *g*-factors were determined from an external standard of γ-irradiated quartz, which has $g = 2.0003$.[87] Attenuation of the microwave power was calibrated on each sample, but 20 dB was the optimal value for all samples.

Solid-state NMR Spectroscopy. 263 GHz/400 MHz DNP solid-state NMR spectroscopy was performed on a commercial Bruker MAS DNP system.[115] The sample temperature was *ca.* 105 K for this system, unless indicated otherwise. A Bruker 3.2 mm MAS DNP probe configured in double resonance mode was used for most experiments. The MAS frequency was 10 kHz and 3.2 mm sapphire rotors were used. Field sweep DNP experiments on glucose and malic acid (Figure 2) and measurements of DNP enhancements for histidine and malonic acid (Figure S2) with the main magnetic field set for optimal negative DNP enhancements were performed with a Bruker 1.3 mm MAS DNP probe[116] configured in double resonance mode. The MAS frequency was 12.5 kHz and 1.3 mm rotors were used. γ-irradiated samples were packed directly into 3.2 mm sapphire or 1.3 mm zirconia rotors without any further modification. Sample preparation for IWI samples followed established procedures.[37-38] Approximately 30 mg of the ground organic solid was impregnated with 15 μL of a 16 mM TEKPOL tetrachloroethane solution.[117] Approximately 30 W and 26.5 W of microwave power was used for γ-irradiated and IWI samples, respectively. $^{1}H \rightarrow ^{13}C$ cross-polarization (CP) contact times of 500 μs was used for all CP experiments. A 90% to 100% linear ramp was used to broaden the Hartmann-Hahn match condition during the ^{1}H spin-lock pulse. Cross polarization radiofrequency fields of approximately 100 and 70 kHz were applied on ^{1}H and ^{13}C, respectively. SPINAL-64 heteronuclear ^{1}H decoupling[118] with a 100 kHz radiofrequency field was applied during ^{13}C signal acquisition. ^{1}H longitudinal relaxation time (T_1) and DNP build-up time (T_{DNP}) constants were measured through ^{13}C-detected CP experiments and fit to a mono-exponential function. Fitting of saturation recovery curves to mono-exponential functions was performed with the relaxation module of the Bruker Topspin 3.6 software. Recycle delays of approximately 1.3 x T_1 were then used for all subsequent CP experiments.

Supplementary Material Available

The supporting information shows proposed structures of radicals, additional EPR and solid-state NMR spectra. Raw NMR data for main text figures and figures showing fits of saturation recovery curves are available at https://doi.org/10.5281/zenodo.5527228.

Acknowledgements

This work was primarily supported by the National Science Foundation under Grant No. 1709972 to A.J.R. We thank Genentech, Inc. and its Innovation Fund, for providing additional financial support for this work. A.J.R. acknowledges additional support from the Alfred P. Sloan Foundation through a Sloan research fellowship. Gamma irradiation of samples at Brookhaven National Lab was supported by the U.S. DOE Office of Science, Division of Chemical Sciences, Geosciences and Biosciences under contract DE-SC0012704. We are grateful to Dr. Paroma Chakravarty and Dr. Lauren Sirois (Genentech Inc.) for providing samples of GDC-022 cocrystals.

References:

1. Maly, T.; Debelouchina, G. T.; Bajaj, V. S.; Hu, K. N.; Joo, C. G.; Mak-Jurkauskas, M. L.; Sirigiri, J. R.; Wel, P. C. van der; Herzfeld, J.; Temkin, R. J.; Griffin, R. G., Dynamic Nuclear Polarization at High Magnetic Fields. *J. Chem. Phys.* **2008,** *128* (5), 052211.
2. Ni, Q. Z.; Daviso, E.; Can, T. V.; Markhasin, E.; Jawla, S. K.; Swager, T. M.; Temkin, R. J.; Herzfeld, J.; Griffin, R. G., High Frequency Dynamic Nuclear Polarization. *Acc. Chem. Res.* **2013,** *46* (9), 1933-1941.
3. Michaelis, V. K.; Ong, T. C.; Kiesewetter, M. K.; Frantz, D. K.; Walish, J. J.; Ravera, E.; Luchinat, C.; Swager, T. M.; Griffin, R. G., Topical Developments in High-Field Dynamic Nuclear Polarization. *Isr. J. Chem.* **2014,** *54* (1-2), 207-221.
4. Lilly Thankamony, A. S.; Wittmann, J. J.; Kaushik, M.; Corzilius, B., Dynamic Nuclear Polarization for Sensitivity Enhancement in Modern Solid-State NMR. *Prog. Nucl. Magn. Reson. Spectrosc.* **2017,** *102-103*, 120-195.
5. Corzilius, B., High-Field Dynamic Nuclear Polarization. *Annu Rev Phys Chem* **2020,** *71*, 143-170.
6. Rossini, A. J.; Zagdoun, A.; Lelli, M.; Lesage, A.; Coperet, C.; Emsley, L., Dynamic Nuclear Polarization Surface Enhanced NMR Spectroscopy. *Acc. Chem. Res.* **2013,** *46* (9), 1942-51.
7. Hope, M. A.; Halat, D. M.; Magusin, P. C.; Paul, S.; Peng, L.; Grey, C. P., Surface-Selective Direct 17O DNP NMR of CeO2 Nanoparticles. *Chem. Commun.* **2017,** *53* (13), 2142-2145.
8. Rossini, A. J., Materials Characterization by Dynamic Nuclear Polarization-Enhanced Solid-State NMR Spectroscopy. *J. Phys. Chem. Lett.* **2018,** *9* (17), 5150-5159.
9. Ravera, E.; Corzilius, B.; Michaelis, V. K.; Rosa, C.; Griffin, R. G.; Luchinat, C.; Bertini, I., Dynamic nuclear polarization of sedimented solutes. *J Am Chem Soc* **2013,** *135* (5), 1641-4.
10. Su, Y.; Andreas, L.; Griffin, R. G., Magic angle spinning NMR of proteins: high-frequency dynamic nuclear polarization and (1)H detection. *Annu Rev Biochem* **2015,** *84*, 465-97.
11. Akbey, U.; Oschkinat, H., Structural biology applications of solid state MAS DNP NMR. *J Magn Reson* **2016,** *269*, 213-224.
12. Fricke, P.; Mance, D.; Chevelkov, V.; Giller, K.; Becker, S.; Baldus, M.; Lange, A., High resolution observed in 800 MHz DNP spectra of extremely rigid type III secretion needles. *J Biomol NMR* **2016,** *65* (3-4), 121-126.
13. Salnikov, E. S.; Aisenbrey, C.; Aussenac, F.; Ouari, O.; Sarrouj, H.; Reiter, C.; Tordo, P.; Engelke, F.; Bechinger, B., Membrane topologies of the PGLa antimicrobial peptide and a transmembrane anchor sequence by Dynamic Nuclear Polarization/solid-state NMR spectroscopy. *Sci Rep* **2016,** *6*, 20895.
14. Jaudzems, K.; Polenova, T.; Pintacuda, G.; Oschkinat, H.; Lesage, A., DNP NMR of biomolecular assemblies. *J Struct Biol* **2019,** *206* (1), 90-98.
15. Pinon, A. C.; Rossini, A. J.; Widdifield, C. M.; Gajan, D.; Emsley, L., Polymorphs of Theophylline Characterized by DNP Enhanced Solid-State NMR. *Mol. Pharm.* **2015,** *12* (11), 4146-53.
16. Ni, Q. Z.; Yang, F.; Can, T. V.; Sergeyev, I. V.; D'Addio, S. M.; Jawla, S. K.; Li, Y.; Lipert, M. P.; Xu, W.; Williamson, R. T.; Leone, A.; Griffin, R. G.; Su, Y., In Situ

Characterization of Pharmaceutical Formulations by Dynamic Nuclear Polarization Enhanced MAS NMR. *J. Phys. Chem. B* **2017,** *121* (34), 8132-8141.

17. Zhao, L.; Pinon, A. C.; Emsley, L.; Rossini, A. J., DNP-Enhanced Solid-State NMR Spectroscopy of Active Pharmaceutical Ingredients. *Magn. Reson. Chem.* **2018,** *56* (7), 583-609.

18. Zhao, Li; Hanrahan, Michael P.; Chakravarty, Paroma; DiPasquale, Antonio G.; Sirois, Lauren E.; Nagapudi, Karthik; Lubach, Joseph W.; Rossini, Aaron J., Characterization of Pharmaceutical Cocrystals and Salts by Dynamic Nuclear Polarization-Enhanced Solid-State NMR Spectroscopy. *Crystal Growth & Design* **2018,** *18* (4), 2588-2601.

19. F. Blanc, L. Sperrin, D. A. Jefferson, S. Pawsey, M. Rosay, C. P. Grey, Dynamic Nuclear Polarization Enhanced Natural Abundance 17O Spectroscopy. *J. Am. Chem. Soc.* **2013,** *135* (8), 2975-2978.

20. Perras, F. A.; Kobayashi, T.; Pruski, M., Natural Abundance 17O DNP Two-Dimensional and Surface-Enhanced NMR Spectroscopy. *J. Am. Chem. Soc.* **2015,** *137* (26), 8336-8339.

21. Bjorgvinsdottir, S.; Walder, B. J.; Pinon, A. C.; Emsley, L., Bulk Nuclear Hyperpolarization of Inorganic Solids By Relay From the Surface. *J. Am. Chem. Soc.* **2018**.

22. Chakrabarty, T.; Goldin, N.; Feintuch, A.; Houben, L.; Leskes, M., Paramagnetic Metal-Ion Dopants as Polarization Agents for Dynamic Nuclear Polarization NMR Spectroscopy in Inorganic Solids. *ChemPhysChem* **2018,** *19* (17), 2139-2142.

23. Li, W.; Wang, Q.; Xu, J.; Aussenac, F.; Qi, G.; Zhao, X.; Gao, P.; Wang, C.; Deng, F., Probing the Surface of gamma-Al2O3 by Oxygen-17 Dynamic Nuclear Polarization Enhanced Solid-State NMR spectroscopy. *Phys Chem Chem Phys* **2018**.

24. Bjorgvinsdottir, S.; Walder, B. J.; Matthey, N.; Emsley, L., Maximizing Nuclear Hyperpolarization in Pulse Cooling under MAS. *J Magn Reson* **2019,** *300*, 142-148.

25. Hu, K. N., Polarizing agents and mechanisms for high-field dynamic nuclear polarization of frozen dielectric solids. *Solid State Nucl Magn Reson* **2011,** *40* (2), 31-41.

26. Can, T. V.; Caporini, M. A.; Mentink-Vigier, F.; Corzilius, B.; Walish, J. J.; Rosay, M.; Maas, W. E.; Baldus, M.; Vega, S.; Swager, T. M.; Griffin, R. G., Overhauser effects in insulating solids. *J Chem Phys* **2014,** *141* (6), 064202.

27. Mathies, G.; Caporini, M. A.; Michaelis, V. K.; Liu, Y.; Hu, K. N.; Mance, D.; Zweier, J. L.; Rosay, M.; Baldus, M.; Griffin, R. G., Efficient Dynamic Nuclear Polarization at 800 MHz/527 GHz with Trityl-Nitroxide Biradicals. *Angew Chem Int Ed Engl* **2015,** *54* (40), 11770-4.

28. Gunther, W. R.; Michaelis, V. K.; Caporini, M. A.; Griffin, R. G.; Roman-Leshkov, Y., Dynamic nuclear polarization NMR enables the analysis of Sn-Beta zeolite prepared with natural abundance (1)(1)(9)Sn precursors. *J Am Chem Soc* **2014,** *136* (17), 6219-22.

29. Jagtap, A. P.; Krstic, I.; Kunjir, N. C.; Hansel, R.; Prisner, T. F.; Sigurdsson, S. T., Sterically shielded spin labels for in-cell EPR spectroscopy: analysis of stability in reducing environment. *Free Radic Res* **2015,** *49* (1), 78-85.

30. Liao, W. C.; Ong, T. C.; Gajan, D.; Bernada, F.; Sauvee, C.; Yulikov, M.; Pucino, M.; Schowner, R.; Schwarzwalder, M.; Buchmeiser, M. R.; Jeschke, G.; Tordo, P.; Ouari, O.; Lesage, A.; Emsley, L.; Coperet, C., Dendritic Polarizing Agents for DNP SENS. *Chem Sci* **2017,** *8* (1), 416-422.

31. Pump, E.; Viger-Gravel, J.; Abou-Hamad, E.; Samantaray, M. K.; Hamzaoui, B.; Gurinov, A.; Anjum, D. H.; Gajan, D.; Lesage, A.; Bendjeriou-Sedjerari, A.; Emsley, L.; Basset, J. M., Reactive Surface Organometallic Complexes Observed Using Dynamic Nuclear Polarization Surface Enhanced NMR Spectroscopy. *Chem. Sci.* **2017,** *8* (1), 284-290.

32. Albert, B. J.; Gao, C.; Sesti, E. L.; Saliba, E. P.; Alaniva, N.; Scott, F. J.; Sigurdsson, S. T.; Barnes, A. B., Dynamic Nuclear Polarization Nuclear Magnetic Resonance in Human Cells Using Fluorescent Polarizing Agents. *Biochemistry* **2018,** *57* (31), 4741-4746.
33. Pump, E.; Bendjeriou-Sedjerari, A.; Viger-Gravel, J.; Gajan, D.; Scotto, B.; Samantaray, M. K.; Abou-Hamad, E.; Gurinov, A.; Almaksoud, W.; Cao, Z.; Lesage, A.; Cavallo, L.; Emsley, L.; Basset, J. M., Predicting the DNP-SENS efficiency in reactive heterogeneous catalysts from hydrophilicity. *Chem Sci* **2018,** *9* (21), 4866-4872.
34. Ha, M.; Thiessen, A. N.; Sergeyev, I. V.; Veinot, J. G. C.; Michaelis, V. K., Endogenous Dynamic Nuclear Polarization NMR of Hydride-Terminated Silicon Nanoparticles. *Solid State Nucl Magn Reson* **2019,** *100*, 77-84.
35. Nagashima, H.; Trebosc, J.; Kon, Y.; Sato, K.; Lafon, O.; Amoureux, J. P., Observation of Low-gamma Quadrupolar Nuclei by Surface-Enhanced NMR Spectroscopy. *J Am Chem Soc* **2020,** *142* (24), 10659-10672.
36. Perras, Frédéric A.; Wang, Lin-Lin; Manzano, J. Sebastian; Chaudhary, Umesh; Opembe, Naftali N.; Johnson, Duane D.; Slowing, Igor I.; Pruski, Marek, Optimal Sample Formulations for DNP SENS: The Importance of Radical-Surface Interactions. *Current Opinion in Colloid & Interface Science* **2018,** *33*, 9-18.
37. Lesage, A.; Lelli, M.; Gajan, D.; Caporini, M. A.; Vitzthum, V.; Mieville, P.; Alauzun, J.; Roussey, A.; Thieuleux, C.; Mehdi, A.; Bodenhausen, G.; Coperet, C.; Emsley, L., Surface Enhanced NMR Spectroscopy by Dynamic Nuclear Polarization. *J. Am. Chem. Soc.* **2010,** *132* (44), 15459-61.
38. Rossini, A. J.; Zagdoun, A.; Hegner, F.; Schwarzwalder, M.; Gajan, D.; Coperet, C.; Lesage, A.; Emsley, L., Dynamic Nuclear Polarization NMR Spectroscopy of Microcrystalline Solids. *J. Am. Chem. Soc.* **2012,** *134* (40), 16899-908.
39. Björgvinsdóttir, Snædís; Moutzouri, Pinelopi; Berruyer, Pierrick; Hope, Michael A.; Emsley, Lyndon, Sensitivity Enhancements in Lithium Titanates by Incipient Wetness Impregnation DNP NMR. *The Journal of Physical Chemistry C* **2020,** *124* (30), 16524-16528.
40. Lock, H.; Wind, R. A.; Maciel, G. E.; Zumbulyadis, N., Si-29 Dynamic Nuclear-Polarization of Dehydrogenated Amorphous-Silicon. *Solid State Communications* **1987,** *64* (1), 41-44.
41. Lee, M.; Cassidy, M. C.; Ramanathan, C.; Marcus, C. M., Decay of nuclear hyperpolarization in silicon microparticles. *Physical Review B* **2011,** *84* (3).
42. Dementyev, A. E.; Cory, D. G.; Ramanathan, C., Dynamic nuclear polarization in silicon microparticles. *Phys Rev Lett* **2008,** *100* (12), 127601.
43. Hayashi, Hiroshi; Itoh, Kohei M.; Vlasenko, Leonid S., Nuclear magnetic resonance linewidth and spin diffusion inS29iisotopically controlled silicon. *Physical Review B* **2008,** *78* (15).
44. Shimon, D.; van Schooten, K. J.; Paul, S.; Peng, Z.; Takahashi, S.; Kockenberger, W.; Ramanathan, C., DNP-NMR of surface hydrogen on silicon microparticles. *Solid State Nucl Magn Reson* **2019,** *101*, 68-75.
45. Wind, R. A.; Duljvestlin, M. J.; Lugt, C. Van Der; Manenschijn, A.; Vriend, J., Applications of Dynamic Nuclear Polarization in 13C NMR in Solids. *Prog in Nucl Magn Reson Spectrosc* **1985,** *17*, 33-67.
46. Wind, Robert A.; Duijvestijn, Michael J.; Lugt, Cees van der; Smidt, Jaap; Vriend, Han, An investigation of coal by means of e.s.r., 1H n.m.r., 13C n.m.r. and dynamic nuclear polarization". *Fuel* **1987,** *66*, 876-885.

47. Bretschneider, C. O.; Akbey, U.; Aussenac, F.; Olsen, G. L.; Feintuch, A.; Oschkinat, H.; Frydman, L., On The Potential of Dynamic Nuclear Polarization Enhanced Diamonds in Solid-State and Dissolution (13) C NMR Spectroscopy. *Chemphyschem* **2016,** *17* (17), 2691-701.
48. Nevzorov, A. A.; Milikisiyants, S.; Marek, A. N.; Smirnov, A. I., Multi-resonant photonic band-gap/saddle coil DNP probehead for static solid state NMR of microliter volume samples. *J Magn Reson* **2018,** *297*, 113-123.
49. Un, S.; Prisner, T.; Weber, R. T.; Seaman, M. J.; Fishbein, K. W.; Mcdermott, A. E.; Singel, D. J.; Griffin, R. G., Pulsed Dynamic Nuclear-Polarization at 5-T. *Chem Phys Lett* **1992,** *189* (1), 54-59.
50. Carver, T. R.; Slichter, C. P., Polarization of Nuclear Spins in Metals. *Physical Review* **1953,** *92* (1), 212-213.
51. Corzilius, B.; Smith, A. A.; Barnes, A. B.; Luchinat, C.; Bertini, I.; Griffin, R. G., High-Field Dynamic Nuclear Polarization With High-Spin Transition Metal Ions. *J. Am. Chem. Soc.* **2011,** *133* (15), 5648-51.
52. Corzilius, B.; Michaelis, V. K.; Penzel, S. A.; Ravera, E.; Smith, A. A.; Luchinat, C.; Griffin, R. G., Dynamic Nuclear Polarization of 1H, 13C, and 59Co in a Tris(ethylenediamine)cobalt(III) Crystalline Lattice Doped with Cr(III). *J. Am. Chem. Soc.* **2014,** *136* (33), 11716-27.
53. Kaushik, M.; Bahrenberg, T.; Can, T. V.; Caporini, M. A.; Silvers, R.; Heiliger, J.; Smith, A. A.; Schwalbe, H.; Griffin, R. G.; Corzilius, B., Gd(iii) and Mn(ii) Complexes for Dynamic Nuclear Polarization: Small Molecular Chelate Polarizing Agents and Applications with Site-Directed Spin Labeling of Proteins. *Phys Chem Chem Phys* **2016,** *18* (39), 27205-27218.
54. Kaushik, M.; Qi, M.; Godt, A.; Corzilius, B., Bis-Gadolinium Complexes for Solid Effect and Cross Effect Dynamic Nuclear Polarization. *Angew Chem Int Ed Engl* **2017,** *56* (15), 4295-4299.
55. Wolf, T.; Kumar, S.; Singh, H.; Chakrabarty, T.; Aussenac, F.; Frenkel, A. I.; Major, D. T.; Leskes, M., Endogenous Dynamic Nuclear Polarization for Natural Abundance (17)O and Lithium NMR in the Bulk of Inorganic Solids. *J Am Chem Soc* **2019,** *141* (1), 451-462.
56. Harchol, A.; Reuveni, G.; Ri, V.; Thomas, B.; Carmieli, R.; Herber, R. H.; Kim, C.; Leskes, M., Endogenous Dynamic Nuclear Polarization for Sensitivity Enhancement in Solid-State NMR of Electrode Materials. *J Phys Chem C Nanomater Interfaces* **2020,** *124* (13), 7082-7090.
57. Jardon-Alvarez, D.; Reuveni, G.; Harchol, A.; Leskes, M., Enabling Natural Abundance (17)O Solid-State NMR by Direct Polarization from Paramagnetic Metal Ions. *J Phys Chem Lett* **2020,** *11* (14), 5439-5445.
58. Paterson, Alexander L.; Perras, Frédéric A.; Besser, Matthew F.; Pruski, Marek, Dynamic Nuclear Polarization of Metal-Doped Oxide Glasses: A Test of the Generality of Paramagnetic Metal Polarizing Agents. *The Journal of Physical Chemistry C* **2020,** *124* (42), 23126-23133.
59. Jardon-Alvarez, D.; Kahn, N.; Houben, L.; Leskes, M., Oxygen Vacancy Distribution in Yttrium-Doped Ceria from (89)Y-(89)Y Correlations via Dynamic Nuclear Polarization Solid-State NMR. *J Phys Chem Lett* **2021,** *12* (11), 2964-2969.
60. Vitzthum, V.; Borcard, F.; Jannin, S.; Morin, M.; Mieville, P.; Caporini, M. A.; Sienkiewicz, A.; Gerber-Lemaire, S.; Bodenhausen, G., Fractional spin-labeling of polymers for enhancing NMR sensitivity by solvent-free dynamic nuclear polarization. *Chemphyschem* **2011,** *12* (16), 2929-32.

61. Lilly Thankamony, Aany Sofia; Lafon, Olivier; Lu, Xingyu; Aussenac, Fabien; Rosay, Melanie; Trébosc, Julien; Vezin, Hervé; Amoureux, Jean-Paul, Solvent-Free High-Field Dynamic Nuclear Polarization of Mesoporous Silica Functionalized with TEMPO. *Applied Magnetic Resonance* **2012,** *43* (1-2), 237-250.
62. Zhang, Y.; Baker, P. J.; Casabianca, L. B., BDPA-Doped Polystyrene Beads as Polarization Agents for DNP-NMR. *J Phys Chem B* **2016,** *120* (1), 18-24.
63. Cao, W.; Wang, W. D.; Xu, H. S.; Sergeyev, I. V.; Struppe, J.; Wang, X.; Mentink-Vigier, F.; Gan, Z.; Xiao, M. X.; Wang, L. Y.; Chen, G. P.; Ding, S. Y.; Bai, S.; Wang, W., Exploring Applications of Covalent Organic Frameworks: Homogeneous Reticulation of Radicals for Dynamic Nuclear Polarization. *J Am Chem Soc* **2018,** *140* (22), 6969-6977.
64. Overall, S. A.; Price, L. E.; Albert, B. J.; Gao, C.; Alaniva, N.; Judge, P. T.; Sesti, E. L.; Wender, P. A.; Kyei, G. B.; Barnes, A. B., In Situ Detection of Endogenous HIV Activation by Dynamic Nuclear Polarization NMR and Flow Cytometry. *Int J Mol Sci* **2020,** *21* (13).
65. Katz, I.; Blank, A., Dynamic Nuclear Polarization in Solid Samples by Electrical-Discharge-Induced Radicals. *J. Magn. Reson.* **2015,** *261*, 95-100.
66. Katz, I.; Feintuch, A.; Carmieli, R.; Blank, A., Proton Polarization Enhancement of up to 150 With Dynamic Nuclear Polarization of Plasma-Treated Glucose Powder. *Solid State Nucl. Magn. Reson.* **2019,** *100*, 26-35.
67. Galindo, S.; Ureña-Nuñez, F.; Urena-Nunez, F., EPR Signal Enhancement of Alanine Irradiated with Thermal Neutrons. *Radiation Research* **1993,** *133* (3).
68. Harbridge, J. R.; Eaton, S. S.; Eaton, G. R., Electron spin-lattice relaxation processes of radicals in irradiated crystalline organic compounds. *J Phys Chem A* **2003,** *107* (5), 598-610.
69. Pauwels, Ewald; Van Speybroeck, Veronique; Vanhaelewyn, Gauthier; Callens, Freddy; Waroquier, Michel, DFT-EPR study of radiation-induced radicals in a-D-glucose. *International Journal of Quantum Chemistry* **2004,** *99* (2), 102-108.
70. Karakirova, Yordanka; Lund, Eva; Yordanov, Nicola D., EPR and UV Investigation of Sucrose Irradiated with Nitrogen Ions and Gamma-rays. *Radiat. Meas.* **2008,** *43* (8), 1337-1342.
71. Aydin, M.; Baskan, M. H.; Osmanoglu, Y. E., EPR Study of Gamma Induced Radicals in Amino and Iminodiacetic Acid Derivatives. *Braz. J. Phys.* **2009,** *39* (3), 583-586.
72. Aydin, M., EPR study of free radicals in amino acid derivatives gamma-irradiated at 300 K. *Indian J Pure Ap Phy* **2010,** *48* (9), 611-614.
73. Raghu, S.; Archana, K.; Sharanappa, C.; Ganesh, S.; Devendrappa, H., Electron beam and gamma ray irradiated polymer electrolyte films: Dielectric properties. *Journal of Radiation Research and Applied Sciences* **2016,** *9* (2), 117-124.
74. Waligorski, M. P. R.; Danialy, G.; Loh, K. S.; Katz, R., The Response of the Alanine Detector after Charged-Particle and Neutron Irradiations. *Appl Radiat Isotopes* **1989,** *40* (10-12), 923-933.
75. Galindo, S.; Klapp, J., EPR of borax-alanine mixtures irradiated with thermal neutrons. *Revista Mexicana De Fisica* **2005,** *51* (2), 193-198.
76. Choi, H.; Kim, J. I.; Lee, B. I.; Lim, Y. K., Application of Alanine/Esr Spectrum Shape Change in Gamma Dosimetry. *Nucl Eng Technol* **2010,** *42* (3), 313-318.
77. Guidelli, E. J.; Ramos, A. P.; Zaniquelli, M. E.; Nicolucci, P.; Baffa, O., Synthesis and characterization of silver/alanine nanocomposites for radiation detection in medical applications: the influence of particle size on the detection properties. *Nanoscale* **2012,** *4* (9), 2884-93.
78. Ciesielski, B., A comment on the article on EPR in silver-alanine nanocomposites for radiation detection by Guidelli et al. in Nanoscale, 4, 2012. *Nanoscale* **2014,** *6* (23), 14570-1.

79. Bartonicek, B.; Kucera, J.; Svetlik, I.; Viererbl, L.; Lahodova, Z.; Tomaskova, L.; Cabalka, M., Extended use of alanine irradiated in experimental reactor for combined gamma- and neutron-dose assessment by ESR spectroscopy and thermal neutron fluence assessment by measurement of (14)C by LSC. *Appl Radiat Isot* **2014,** *93*, 52-6.
80. Abraham, M.; McCausland, M. A. H.; Robinson, F. N. H., Dynamic Nuclear Polarization. *Physical Review Letters* **1959,** *2* (11), 449-451.
81. Lushchikov, V. I.; Manenkov, A. A.; Taran, Y. V., Dynamic Polarization of Protons in Neutron Irradiated Polyethylene. *Phys. Solid State* **1962,** *3* (11), 2541-2544.
82. Kessenikh, A. V.; Manenkov, A. A.; Pyatnitskii, G. I., On Explanation of Experimental Data On Dynamic Polarization of Protons in Irradiated Polyethylenes. *Sov Phys-Sol State* **1964,** *6* (3), 827-830.
83. Hill, D. A.; Hasher, B. A.; Hwang, C. F., Dynamic Polarization of Protons in Radiation-Damaged Polyethylene by the Solid Effect. *Phys. Lett.* **1966,** *23* (1), 63-64.
84. Burget, J.; Petricek, V.; Sacha, J.; Tichy, R., Dynamic Polarization of Protons in Irradiated Polymers. *Czech. J. Phys.* **1967,** *17* (11), 1041-&.
85. Carnahan, S. L.; Venkatesh, A.; Perras, F. A.; Wishart, J. F.; Rossini, A. J., High-Field Magic Angle Spinning Dynamic Nuclear Polarization Using Radicals Created by gamma-Irradiation. *J Phys Chem Lett* **2019,** *10* (17), 4770-4776.
86. Perras, F. A.; Raju, M.; Carnahan, S. L.; Akbarian, D.; van Duin, A. C. T.; Rossini, A. J.; Pruski, M., Full-Scale Ab Initio Simulation of Magic-Angle-Spinning Dynamic Nuclear Polarization. *J Phys Chem Lett* **2020,** *11* (14), 5655-5660.
87. Weeks, R. A.; Nelson, C. M., Irradiation Effects and Short-Range Order in Fused Silica and Quartz. *J. Appl. Phys.* **1960,** *31* (9), 1555-1558.
88. Eaton, S. S.; Eaton, G. R., Irradiated Fused-Quartz Standard Sample for Time-Domain Epr. *J. Magn. Reson.* **1993,** *102* (3), 354-356.
89. Schoepfle, C. S.; Fellows, C. H., Gaseous products from action of cathode rays on hydrocarbons. *Ind Eng Chem* **1931,** *23*, 1396-1398.
90. Cook, J. B.; Elliott, J. P.; Wyard, S. J., Electron spin resonance of an irradiated single crystal of maleic acid. *Molecular Physics* **1967,** *12* (2), 185-195.
91. Eda, Bunzo; Iwasaki, Machio, E.S.R. study of the electron trapping centre in a single crystal of maleic acid irradiated at 77 K. *Molecular Physics* **1972,** *24* (3), 589-595.
92. Saxebol, G.; Sagstuen, E., Radiation damage in L-histidine-HCl monohydrate. *Int J Radiat Biol Relat Stud Phys Chem Med* **1974,** *26* (4), 373-82.
93. Tezel, Ozden; Koroglu, Ahmet; Tapramaz, Recep, ESR of Gamma Irradiated C2H2O4.2H2O Single Crystal. *Spectroscopy Letters* **2000,** *33* (5), 735-742.
94. McCalley, R. C.; Kwiram, Alvin L., ENDOR studies at 4.2 K of the radicals in malonic acid single crystals. *The Journal of Physical Chemistry* **2002,** *97* (12), 2888-2903.
95. Benchaabane, Hafidha S.; Ozer, Yekta A.; Özalp, Meral; Kilic, Ekrem; Polat, Mustafa; Korkmaz, Mustafa, Gamma Radiation Studies on Sulfathiazole (Powder and Model-Ophthalmic Solution). *FABAD J. Pharm. Sci.* **2003,** *28*, 93-106.
96. Harbridge, J. R.; Eaton, S. S.; Eaton, G. R., Electron Spin Relaxation of Radicals in T-Irradiated Malonic Acid and Methyl Malonic Acid. *Appl. Magn. Reson.* **2003,** *24*, 261-276.
97. Başkan, M. Halim; Aydın, Murat; Osmanoğlu, Şemsettin, Investigation of 60Co γ-irradiated l-(−) malic acid, N-methyl-dl-valine and l-glutamic acid γ-ethyl ester by electron paramagnetic resonance technique. *Journal of Molecular Structure* **2010,** *983* (1-3), 200-202.

98. Marciniec, Barbara; Stawny, Maciej; Olszewski, Karol; Kozak, Maciej; Naskrent, Marek, Analytical study on irradiated methylxanthine derivatives. *Journal of Thermal Analysis and Calorimetry* **2012,** *111* (3), 2165-2170.
99. Ramos, Paweł; Pilawa, Barbara, Electron Paramagnetic Resonance Examination of Free Radical Formation in Salicylic Acid and Urea Exposed to UV Irradiation. *International Journal of Photoenergy* **2016,** *2016*, 1-7.
100. Ramos, Paweł; Pilawa, Barbara, Free radical formation in salicylic acid and heating parameters – application of EPR, UV-Vis, TGA and colorimetry examination to optimize thermal sterilization. *Acta Poloniae Pharmaceutica - Drug Research* **2020,** *77* (3), 431-441.
101. Caliskan, Betul; Caliskan, Ali Cengiz, Electron paramagnetic resonance study of the paramagnetic centers in gamma-irradiated oxalic acid dihydrate single crystal. *Radiation Physics and Chemistry* **2021,** *188*.
102. Burton, Milton, Radiation Chemistry. *J Phys Chem* **1947,** *51* (2), 611-625.
103. Baidak, A.; Badali, M.; LaVerne, J. A., Role of the low-energy excited states in the radiolysis of aromatic liquids. *J Phys Chem A* **2011,** *115* (26), 7418-27.
104. LaVerne, J. A.; Dowling-Medley, J., Combinations of Aromatic and Aliphatic Radiolysis. *J Phys Chem A* **2015,** *119* (40), 10125-9.
105. Mentink-Vigier, F.; Barra, A. L.; van Tol, J.; Hediger, S.; Lee, D.; De Paepe, G., De novo prediction of cross-effect efficiency for magic angle spinning dynamic nuclear polarization. *Phys Chem Chem Phys* **2019,** *21* (4), 2166-2176.
106. Hanrahan, M. P.; Venkatesh, A.; Carnahan, S. L.; Calahan, J. L.; Lubach, J. W.; Munson, E. J.; Rossini, A. J., Enhancing the resolution of (1)H and (13)C solid-state NMR spectra by reduction of anisotropic bulk magnetic susceptibility broadening. *Phys Chem Chem Phys* **2017,** *19* (41), 28153-28162.
107. Pinon, Arthur C.; Schlagnitweit, Judith; Berruyer, Pierrick; Rossini, Aaron J.; Lelli, Moreno; Socie, Etienne; Tang, Mingxue; Pham, Tran; Lesage, Anne; Schantz, Staffan; Emsley, Lyndon, Measuring Nano- to Microstructures from Relayed Dynamic Nuclear Polarization NMR. *J. Phys. Chem. C* **2017,** *121* (29), 15993-16005.
108. Lelli, M.; Chaudhari, S. R.; Gajan, D.; Casano, G.; Rossini, A. J.; Ouari, O.; Tordo, P.; Lesage, A.; Emsley, L., Solid-State Dynamic Nuclear Polarization at 9.4 and 18.8 T from 100 K to Room Temperature. *J Am Chem Soc* **2015,** *137* (46), 14558-61.
109. Hope, Michael A.; Björgvinsdóttir, Snædís; Halat, David M.; Menzildjian, Georges; Wang, Zhuoran; Zhang, Bowen; MacManus-Driscoll, Judith L.; Lesage, Anne; Lelli, Moreno; Emsley, Lyndon; Grey, Clare P., Endogenous 17O Dynamic Nuclear Polarization of Gd-Doped CeO2 from 100 to 370 K. *The Journal of Physical Chemistry C* **2021,** *125* (34), 18799-18809.
110. Thurber, K. R.; Yau, W. M.; Tycko, R., Low-temperature dynamic nuclear polarization at 9.4 T with a 30 mW microwave source. *J Magn Reson* **2010,** *204* (2), 303-13.
111. Matsuki, Y.; Ueda, K.; Idehara, T.; Ikeda, R.; Ogawa, I.; Nakamura, S.; Toda, M.; Anai, T.; Fujiwara, T., Helium-cooling and -spinning dynamic nuclear polarization for sensitivity-enhanced solid-state NMR at 14 T and 30 K. *J Magn Reson* **2012,** *225*, 1-9.
112. Lee, D.; Bouleau, E.; Saint-Bonnet, P.; Hediger, S.; De Paepe, G., Ultra-low temperature MAS-DNP. *J Magn Reson* **2016,** *264*, 116-124.
113. Thurber, K.; Tycko, R., Low-temperature dynamic nuclear polarization with helium-cooled samples and nitrogen-driven magic-angle spinning. *J Magn Reson* **2016,** *264*, 99-106.

114. Sesti, E. L.; Alaniva, N.; Rand, P. W.; Choi, E. J.; Albert, B. J.; Saliba, E. P.; Scott, F. J.; Barnes, A. B., Magic angle spinning NMR below 6K with a computational fluid dynamics analysis of fluid flow and temperature gradients. *J Magn Reson* **2018,** *286*, 1-9.
115. Rosay, M.; Tometich, L.; Pawsey, S.; Bader, R.; Schauwecker, R.; Blank, M.; Borchard, P. M.; Cauffman, S. R.; Felch, K. L.; Weber, R. T.; Temkin, R. J.; Griffin, R. G.; Maas, W. E., Solid-State Dynamic Nuclear Polarization at 263 GHz: Spectrometer Design and Experimental Results. *Phys. Chem. Chem. Phys.* **2010,** *12* (22), 5850-60.
116. Chaudhari, S. R.; Berruyer, P.; Gajan, D.; Reiter, C.; Engelke, F.; Silverio, D. L.; Coperet, C.; Lelli, M.; Lesage, A.; Emsley, L., Dynamic nuclear polarization at 40 kHz magic angle spinning. *Phys Chem Chem Phys* **2016,** *18* (15), 10616-22.
117. Zagdoun, A.; Casano, G.; Ouari, O.; Schwarzwalder, M.; Rossini, A. J.; Aussenac, F.; Yulikov, M.; Jeschke, G.; Coperet, C.; Lesage, A.; Tordo, P.; Emsley, L., Large molecular weight nitroxide biradicals providing efficient dynamic nuclear polarization at temperatures up to 200 K. *J Am Chem Soc* **2013,** *135* (34), 12790-7.
118. Fung, B. M.; Khitrin, A. K.; Ermolaev, K., An improved broadband decoupling sequence for liquid crystals and solids. *J Magn Reson* **2000,** *142* (1), 97-101.